A new Heat release rate (HRR) law for Homogeneous Charge Compression Ignition (HCCI) combustion mode

Miguel Torres García; Francisco José Jiménez-Espadafor Aguilar; Tomás Sánchez Lencero; José Antonio Becerra Villanueva.*

Thermal Power Group, Department of Energy Engineering. University of Seville. Escuela Técnica Superior de Ingenieros de Sevilla. Camino de los Descubrimientos, s/n. 41092 Sevilla, España.

*Corresponding author. Tel.:+34954486111; fax: +34954487243. E-mail: miguel_torres@esi.us.es (Miguel Torres García)

Abstract

Homogeneous charge compression ignition (HCCI) engines are drawing attracting attention as the next-generation's internal combustion engine, mainly because of its very low NOx and soot emissions and also for improvement in engine efficiency. Much research has been carried out in order to go deeper in this combustion process using multizone models or CFD codes. These simulation tools, although they can give a detailed view of the combustion process, are very time consuming and the results depend a lot on the initial conditions. A previous step to be considered in the simulation of the HCCI process is a heat release law evaluated from results of the experiment and a zero dimensional model. This paper focuses on the development of a new heat release rate (HRR) law that models the HCCI process when the combustion chamber is considered as a homogeneous volume. The parameters of this law have been adjusted through an optimization process that has allowed to fit the combustion chamber

pressure. All the engine operative conditions from low to full load have been successfully simulated with this HRR law, with the maximum error in the estimation of combustion chamber pressure less than 2%.

Keywords: HRR (heat release rate); EGR (exhaust gas recirculation); HCCI (homogeneous charge compression ignition), in-cylinder NO_x.

Nomenclature

$\overline{S}_p$	Mean piston speed (m/s)
A_c	Common area of heat transfer
a_1, a_2	Shape factors for HRR
ATDC	After top dead center
BDC	Bottom dead center
BTDC	Before top dead center
C_1, C_2	Constants
CFD	Computational Fluid Dynamics
CO_2	Carbon dioxide
DI	Direct injection
EGR	Exhaust Gas Recirculation
H_2O	Water
h_c	Heat transfer coefficient

HCCI	Homogeneous Charge Compression Ignition
HRR	Heat Release Rate
K_1, K_2	Terms of HRR law
LHV	Lower Heat Value
$\dot{m}$	Mass flow (kg/s)
M_p, M_{pp}	Shape factors
P,p	Pressure (bar)
Q	Heat (J)
Q_p	Heat release in HCCI combustion mode (J)
Q_W	Wall heat loss (J)
RPM	Revolutions per minute
SI	Spark ignition
T	temperature (K)
TDC	Top dead center
T_g	Gas temperature (K)
T_W	Cylinder wall temperature (K)
V	Volume (m^3)
V_d	Displacement
W	Power (W)
Greek letter	
θ	Crankshaft angle (radians)
θ_p	Duration of the energy release (radians)

Φ	fuel-air equivalence ratio
ω	Angular speed (rad/s)
$\alpha_{scaling}$	Scaling factor

1. INTRODUCTION

The auto-ignition combustion of homogeneous air-diesel fuel mixtures (HCCI) is a technology with great potential in NO_x and soot emission reduction [1]. It is based on self ignition of a homogenous air-diesel fuel mixture without an external ignition source. At present, there is not an analytical function for modelling the heat release rate in HCCI combustion mode which hinders the combustion analysis and makes the development of intensive tests and CFD calculus necessary. Gas temperature is very important in the start of combustion and chemical kinetics. For this reason, heat transfer inside the combustion chamber has a significant role in HCCI combustion mode. Much research activity has been carried out on global heat transfer models, e.g. Annand[2], Woschnic[3] or Hohenberg[4], which have been elaborated in engine conditions that vary significantly from those in HCCI combustion.

The dominant heat transfer mechanism in HCCI combustion mode is forced convection from hot gases to the combustion chamber walls. Due to very low soot formation and relatively low bulk gas temperature, the radiation effect is very small, the opposite being the case in the conventional diesel combustion mode. For this reason, any HRR analysis for HCCI combustion mode should be developed through a dedicated heat transfer model. In this paper, that of Junseok Chang has been used [5].

Regarding the rate of heat release in HCCI combustion mode, it is not controlled by the rate of fuel injection as in DI engines, nor by finite turbulent flame propagation as in SI engines. The absence of an ignition control mechanism has led researchers to explore a range of control strategies. Performing these explorations solely in the laboratory would be inefficient, expensive, and impractical since there are many variables that exhibit complex interaction. Fundamental tools, such as computational fluid dynamics codes (CFD) with detailed chemistry, need to be applied in order to provide insight into the combustion process. Codes of this nature are very computationally intensive and usually require some simplifications to expedite the solution while attempting to maintain accuracy. Fully coupled CFD/kinetic models have employed a number of different combustion methodologies. Kusaka [6] had no explicit modification of the reaction rate due to mixing; the only mixing that occurred during combustion was that normally calculated by the CFD code. Results with a detailed kinetic scheme showed a more rapid combustion event than the experiment. Because of the relatively coarse grid that was used, there is the possibility that the mass in colder zones was underestimated. Kong et al. (2001) [7] coupled the KIVA-3V CFD code with kinetics modified for turbulence effects and found a similar effect; i.e., when no turbulence effect was used, they predicted a higher energy release rate than was seen in the experiment. All these models present a severe drawback: the huge computational load that precludes efficient and quick analysis of the HCCI process. In this paper, a theory-experimental model is developed which allows evaluating the HRR in HCCI combustion mode in a modified diesel engine (DEUTZ-DITER FL1 906) from an analytical law of HRR. In all experimental studies carried out on HCCI combustion mode, it is observed that the

HRR is quite different from the one in diesel combustion mode. The HRR of the HCCI process presents only a premixed combustion shape while that of the diesel mode shows premixed and diffusive appearance combustion. The knowledge of an analytical HRR law validated in a wide range of operating conditions in HCCI combustion mode will be a great advance in knowledge of HCCI combustion and could allow developing a predictive computational model for this combustion process.

This paper develops a new heat release rate (HRR) law that models the HCCI process. The parameters of this law have been adjusted through an optimization process that has allowed to fit the combustion chamber pressure. The paper is organised as follows:

- Engine experimental setup, where the test rig and experimental procedure is described.
- Model for the evaluation of the HRR. Here the model developed for HRR from experimental measurement is explained.
- Analytical law for HRR in HCCI combustion mode, where the new HRR is presented.
- Numerical solution procedure.
- Results and conclusions.

2. ENGINE AND EXPERIMENTAL SETUP

The experimental part of this work is based on the tests carried out on the modified DEUTZ FL1 906 engine. The original diesel engine was modified to adapt it to HCCI combustion. The main characteristics of the engine are shown in Table 1 and the experimental installation is represented in Figure 1. The modified engine systems were:

1º Injection System: the injection pump was extracted from the engine block, and its design modified to control the injection point. The gear of the crankshaft coupling to the injection pump was substituted by a transmission belt.

2º Exhaust gas recirculation system (EGR): an EGR system was designed which included an exhaust gases refrigeration system. With this system, the EGR by-passed mass fraction and the temperature of the recirculated gases can be controlled.

3º Measurement equipment: different sensors were located in the engine to monitor the pressure in the combustion chamber, the injection pressure, needle rising, engine speed, exhaust temperature, fuel mass flow, the intake system, pressure evolution, temperature and air mass flow.

Figure 1

Start of combustion is highly dependent on intake temperature. To carry out a full analysis of the intake temperature effect in different operating conditions, a heating system for the intake air was designed (figure 1). Also, a heat exchanger cooler for the EGR gases was installed to control the recirculated gases temperature and so to control the temperature of the cylinder intake mixture. The installation incorporates stagnation boxes to eliminate the strong pulsating waves of the mono-cylinder engine.

Table 1

Tests were done with a commercial diesel fuel compatible with European Standard EN590. The recirculated gases (EGR) were cooled in order to control the intake temperature that never surpassed the ambient temperature. The external EGR rate is

evaluated measuring the EGR mass recirculated and the total mass inlet. The formula is as follows:

$$EGR(\%mass) = \frac{\dot{m}_{EGR}}{\dot{m}_{EGR} + \dot{m}_{Air}} \cdot 100 \quad (1)$$

where $\dot{m}_{EGR}$ and $\dot{m}_{Air}$ are measured with a hot wire flow meter

3. MODEL FOR THE EVALUATION OF THE HRR

In this work, a thermodynamic zero-dimensional model has been used to carry out the analysis and evaluation of the parameters of an analytical law of HRR, following an iterative optimization process. The combustion chamber is considered as a perfect mixture reactor with variable volume, with even pressure distribution, temperature and concentration of chemical species (see Figure 2) with heat losses. Equations and simplifications that govern the mathematical model are needed due to complex interaction between physics and chemical phenomenon during combustion and are described in the following equations [8]:

Figure 2

- Thermal state equation
- Combustion chamber volume
- First Principle of Thermodynamics[9]
- Heat losses
- Blow by has not been considered.

The heat loss model is written as follows:

$$\frac{dQ_W}{d\theta} = A_c h_c \left(T_g - T_W\right)\frac{1}{\omega} \tag{2}$$

The heat transfer coefficient h_c (W/m^2 K) is based on the correlation formula given by Junseok Chang [5]. Q_W is the wall heat loss, A_c is the area in contact with the gases, T_g(K) is the gas temperature, T_w(K) is the cylinder wall temperature and ω (rad/s) is the average angular speed. The global heat transfer coefficient can be written as:

$$h_c(t) = \alpha_{scaling} L(t)^{-0.2} p(t)^{0.8} T(t)^{-0.73} v(t)^{0.8} \tag{3}$$

A scaling factor $\alpha_{scaling}$ is used for tuning of the coefficient to match specific engine geometry. Combustion-induced gas velocity is a function of the difference between motoring and firing pressure [10].

$$v(t) = C_1 \overline{S}_p + \frac{C_2}{6}\frac{V_d T_r}{p_r V_r}\left(p - p_{motoring}\right) \tag{4}$$

The main idea for using this equation is to keep the velocity constant during the unfiring period of the cycle, and to then impose a steep velocity rise once combustion pressure departs from motoring pressure. The subscript r denotes a reference crank angle, such as intake valve closing.

Figure 3 shows the net cumulative heat release obtained from a fuel consumption of 0.015 g/cycle, 1800 RPM and 0% EGR. Combustion efficiency comes from measured exhaust gas composition, 93-96%, so the energy released by the fuel per cycle (LHV=42.5 MJ/kg) is between 593-612J. Crevice losses are considered very low [5], about 2%. Parameter $\alpha_{scaling}$ from equation (3) has been tuned so that the cumulative heat released by fuel plus heat losses, plus 2% from crevices, is equal to the energy

released by the fuel. This analysis was repeated over the whole range of operating conditions tested.

Figure 3

In the experimental results there is no kinetic information, therefore the start of combustion is defined from the Heat Release Rate (HRR) obtained from the registered in-cylinder pressure combined with a zero-dimensional model of the combustion system: the combustion starts when the cumulative energy released is 5% of the total [10, 11]. The combustion duration has been established as the angle between the start of combustion and that corresponding to 10% of the magnitude of the peak of HRR on the falling side of the curve [12].

3.1 HRR ANALYSIS

In general, cold EGR plays a significant role on HCCI combustion characteristics. As shown in Figure 4, the maximum in-cylinder pressure decreases, the ignition delay increases, the peak value of HRR diminishes and the combustion process is prolonged with the introduction of cold external EGR. The increment of ignition delay diminishes the amount of fuel burned before TDC, which reduces the maximum combustion pressure. Also, the temperature of the gases is lower, which decelerates the combustion process. Although combustion is prolonged with any increment of the EGR rate, which makes that combustion process separate from constant volume combustion, the specific fuel consumption improves at the end. In Figure 4, any increment of EGR produces an increment of engine torque due to a reduction of the fuel burned and, therefore, of the pressure BTDC up to a threshold level that the torque reduces. This is associated with

lack of oxygen, that is, more than about 20% of EGR to 2100 RPM reduces the inlet air and so there is not enough oxygen to burn the fuel.

Figure 4

Figure 5 shows the combustion ignition angle and combustion duration versus EGR rate for different fuel consumption. In both images, two different zones can be clearly seen: from 0 to 25% EGR and from this to the end. In the first part, the combustion duration and ignition angle change slightly and almost linearly with the EGR rate, but in the second zone the changes are more intense with EGR rate, which can be explained by the reduction in charge temperature and probably by the lack of air that decelerates the combustion rate.

Figure 5

According to chemical kinetics of HCCI combustion [13-16], combustion characteristics are dominated by the low and middle temperature reaction mechanism. With an increase of cold EGR rate, the mixture temperature rising rate during the compression process decreases because of the increase of heat capacity. Also, the oxidation and decomposition reaction rate were depressed for the final products such as CO_2, NO_x, and H_2O.

4. ANALITICAL LAW FOR HRR IN HCCI COMBUSTION MODE

The HRR curves shown in Figure 4 reveal the very high heat release rate that causes a rapid increase in pressure in the engine cylinder. From this, combustion is characterized by the sudden steep pressure rise on the cylinder pressure curve and the peak on the HRR. Once all the already formed flammable mixture is burned, the HRR decreases

until the end of combustion. For all fuel consumption rates, engine speeds and EGR rates tested in HCCI mode, the HRR has shown the same development.

Therefore, combustion is completely controlled by chemical kinetics. Because gas cylinder temperature is not sufficiently high, the fuel does not reach pyrolysis conditions almost avoiding soot formation and diminishing NO_x formation drastically [17].

A model for the HRR that can be adapted efficiently to a combustion process controlled only by chemical kinetics is that of Wiebe. In this work, it has been found that modifying the Wiebe function has allowed the formulation of a new HRR law that fits quite well with the HCCI combustion process [18].

$$\frac{dQ}{d\theta} = a_1 \frac{Q_p}{\theta_p}(M_p + 1)\left(\frac{\theta}{\theta_p}\right)^{M_p} \exp\left[-a_2\left(\frac{\theta}{\theta_p}\right)^{M_{pp}+1}\right] \qquad (5)$$

Where a_1, a_2, M_p, M_{pp} are shape factors. In order to reproduce the HRR the parameter M_p has had to be considered different from the parameter M_{pp}, see (5). M_p has been considered as a different parameter from M_{pp} (the opposite of the original Wiebe function), θ_p is the duration of the energy release, and Q_p characterizes the heat release in HCCI combustion mode.

Defining the terms:

$$K_1 = a_1 \frac{Q_p}{\theta_p^{M_p+1}}\left(M_p + 1\right) \qquad K_2 = a_2 \frac{1}{\theta_p^{M_{pp}+1}} \qquad (6)$$

It follows that the HRR is:

$$\frac{dQ}{d\theta} = K_1 \theta^{M_p} \exp\left[-K_2 \theta^{M_{pp}+1}\right] \qquad (7)$$

5. NUMERICAL SOLUTION PROCEDURE

Once the HRR law has been chosen, the problem is the identification of values of the parameters of this law, K_1, K_2, M_p, M_{pp} for each operative engine condition. Finding the values of the sought parameters is an optimization problem that can be formulated as:

- Minimize L

$$L = \sum_{i=1}^{n} \varepsilon_i^2 = \sum_{i=1}^{n} \left(P_{\exp erimental}(\theta_i) - P_{simulated}(\theta_i, K_1, K_2, M_p, M_{pp}) \right)^2 \quad (8)$$

Where ε_i is a measure of the error, $P_{experimental}$ and $P_{simulated}$ are the measured and simulated combustion chamber pressure respectively, and θ_i is every crank angle where pressure is measured and simulated.

5.1 EVALUATION OF THE COMBUSTION CHAMBER PRESSURE FROM HRR LAW.

Combustion pressure, $P_{simulated,}$ is evaluated through a zero zone model which includes the following submodels:

- Thermal state equation
- Combustion chamber volume
- Heat release rate law
- First principle of thermodynamic
- Start of combustion model [19]
- Heat losses[5]

The equations of the thermodynamic model presented are solved numerically step-by-step using a simple time marching technique, and they give the combustion chamber pressure, $P_{simulated}$.

The kinetic chemical model is based on a replacement fuel (PRF) fuel to provide the beginning of combustion. The start of combustion, or ignition point, is controlled by physical processes, such as the atomization of the fuel, fuel evaporation and fuel –air mix, and by the chemical kinetic reactions among the fuel, air and combustion products [19]. The direct simulation of the oxidation reactions of commercial diesel fuel is unavailable due to its composition, formed by thousands of chemical species, and the uncertainty of some mechanisms of oxidation. So commercial fuel is usually modelled on a PRF of a well-known composition and kinetic mechanisms [20].

5.2 OPTIMIZATION PROCESS

The scheme of the numerical solution procedure is represented in Figure 6. The theory-experimental model is a direct type, the start is the pressure chamber curve and the end is the HRR curve. The time of computation can be raised because, during the optimization process, a direct model has to be resolved in every iteration and the rate of convergence depends on the initial conditions used and the accuracy. One of the most decisive factors in computation time is the initial condition.

Figure 6

6. RESULTS AND DISCUSSION

With the new HRR law, the optimized parameters have allowed good concordance between experimental and combustion pressure chamber simulations. Figure 7 compares simulated cylinder pressures, obtained as discussed in previous sections, with measured ones, derived from the experimental study. The modelled cylinder pressure shown has been obtained from the new HRR law for different mass flow and EGR; the angular velocity is 1800 RPM and the fuel consumption is constant (1.3e-5 kg/cycle).

In terms of the area under the pressure curve between IVC and EVO, the error is about 1%. An interesting aspect to highlight is the good reproduction of pressure during the combustion process, that is, when an abrupt increase of pressure takes place.

Figure 7

Table 2 shows the four parameters of the new HRR law for quite different operating engine conditions.

Table 2

Figures 8 and 9 show the measured and predicted cylinder pressures and the heat release rate obtained from the new HRR law. The results show good concordance between experimental and numerical results; both the angular velocity and fuel consumption are constant. As can be observed, the new HRR law adapts perfectly to any load condition. From the minimum EGR rate (5%), each increment of the EGR rate has three effects on the HRR

a) A delay in start of combustion.
b) A diminution of the maximum heat release rate.
c) An increase of combustion duration.

From Table 3 and for engine conditions in Figure 9 it can be observed that every EGR increment also increases engine torque. The increase of torque is due to the diminution of combustion pressure during the compression stroke because of the delay in start of combustion, effect a. Because of this power increase at the same engine speed and fuel consumption, there is also an improvement in the engine's specific fuel consumption to weight of effect c that reduces thermodynamic efficiency [21]. Effect b produces a diminution of the combustion chamber temperature and so there will be a diminution of NO_x emissions [22].

Figure 8

Figure 9

Table 3 quantifies the error between measurement and simulation built from the new HRR law. The difference between maximum pressure measured and predicted is less than 0.8%, the error of the area under cylinder pressure is less than 2% but is reduced to 1.4% when cylinder pressure is between inlet valve opening (IVO) and exhaust valve closing (EVC).

Table 3

7. CONCLUSIONS

In this work, an experimental and simulation study has been carried out to compare the performance of a new HRR law that defines a proportion of slower combustion for HCCI engine modelling. The new HRR law was implemented in an engine model to evaluate performance in comparison to the experimental data obtained in detailed tests.

The study showed that by describing a proportion of slower combustion with the new HRR proposed, it was possible to achieve a very good match to experimental data. The new HRR law allows predicting the cylinder pressure curve perfectly with minimum error. As has been shown, the HRR law depends on four parameters that can be related

to any load condition. Research is in progress on the development of a predictive model of the engine in HCCI combustion mode.

ACKNOWLEDMENTS

The work in this paper is a part of item CTQ2007-68026-CO2-02/PPQ within the I+D+i national plan in the period 2007-2009 and has been supported by the Spanish Government (Ministry of Science and Education). The authors are grateful to the Ministry of Science and Education of Spain for their financial support of this work.

REFERENCES

1. Thring. R.H. "Homogeneous Charge Compression Ignition (HCCI) Engines." SAE Paper No.892068.
2. Annand. W.J.D. (1963). "Heat transfer in the Cylinders of Reciprocating Engines." Proc. Inst. Mech. Engrs. Vol. 177. No. 36.
3. Woschni. G. (1967). "Equation for the Instantaneous Heat Transfer Coefficient in the Internal Combustion Engine" SAE Paper 670931.
4. Hohenberg. G.F. "Advanced Approaches for Heat Transfer Calculations". SAE Paper 790825.
5. Junseok Chang et al. "New heat Transfer Correlation for an HCCI engine derived from measurements of instantaneous surface heat flux". Sae Paper 2004-01-2996.
6. Kusaka. J. et al. (1999) "Predicting Homogeneous Charge Compression Ignition Characteristic of various Hydrocarbons." Proceeding of the 15th Internal Combustion Engine Symposium (International). Seoul. Korea (1999).

7. Kong. S-C. and Reitz. R.D. (2000). "Use of Detailed Chemical Kinetics to Study HCCI Engine Combustion with Consideration of Turbulent Mixing Effects." Paper 2000-ICE-306. Proceeding of ASME-ICE Fall Technical Conference. ICE-Vol.35-1.
8. C.D. Rakopoulos, K.A Antonopoulos, D.C. Rakopoulos. Experimental heat release analysis and emissions of a HSDI diesel engine fuelled with ethanol-diesel fuel blends. Energy 32(2007), 1791-1808.
9. Heywood. J.B. "Internal Combustion Engine Fundamentals". Ed. McGraw-Hill Book Company. Singapur (Singapur). 1998.
10. Lü Xingcai. Chen Wei. Ji Libin. Huang Zhen. The effects of external exhaust Gas recirculation and Cetane number improver on the gasoline homogeneous charge compression ignition engines. Combust. Sci. and Tech.. (2006) 178:1237-1249.
11. Huber. K. Woschni. G. Zeilinger. K. "Investigations on Heat Transfer in Internal Combustion Engines under Low load and motoring conditions". SAE Paper 905018.
12. Lü Xingcai. Hou Yuchun. Ji Libin. Zu Linlin. and Huang Zhen. Heat Release Analysis on Combustion and Parametric Study on Emissions of HCCI Engines Fuelled with 2-Propanol/n-Heptane Blend Fuels. Energy and Fuels 20(2006). 1870-1878.
13. Daeyup Lee and Shinichi Goto. (Mechanical Engineering Laboratory MITI) "Chemical Kinetic Study of a Cetane Number Enhancing Additive for an LGP DI Diesel Engine." SAE Paper 2000-01-0193.

14. Lei Shi et al. Study of low emission homogeneous charge compression ignition (HCCI) engine using combined internal and external exhaust gas recirculation (EGR). Energy 31(2006). 2665-2676.
15. Curran. H. J. Gaffuri. P. Pitz. W. J. and Westbrook. C. K. "A Comprehensive Modeling Study of n-Heptane Oxidation" Combustion and Flame 114(1998):149-177
16. Curran. H. J. Gaffuri. P.Pitz. W. J.and Westbrook. C. K. "A Comprehensive Modeling Study of iso-Octane Oxidation" Combustion and Flame 129(2002):253-280
17. Zhijun Peng. Hua Zhao. Tom Ma. Nicos Ladommatos. “Characteristic of Homogeneous charge Compression Ignition (HCCI) combustion and Emissions of n-Heptane.” Combust. Sci. and Tech. 177(2005):2113-2150.
18. H.Yasar, H.S. Soyhan, H. Walmsley, B. Head, C. Sorusbay. Double-Wiebe function: An approach for single-zone HCCI engine modeling. Applied thermal Engineering 28 (2008) 1284-1290.
19. Torres Garcia. M.; Chacartegui Ramirez. R.; Jimenez-Espadafor Aguilar. F; Sanchez Lencero. Analysis of the Start of Combustion of a Diesel Fuel in a HCCI Process through an Integral Chemical Kinetic Model and Experimentation. Energy & Fuels (2008). Vol 22(2), pp 987-995
20. Richter M. et al. The Influence of charge Inhomogeneity on the HCCI Combustion Process. SAE Technical Paper (2000) 2000-01-2868.
21. Yoshiaki Nishijima. Yasou Asaumi and Yuzo Aoyagi. Premixed Lean Diesel Combustion (PREDIC) using Impingement Spray System. New ACE Institute Co. Ltd. SAE Paper (2001) 2001-01-1892.

22. Y Murata. J Kusaka. M Odaka. Y Daisho. D Kawako. H Susuki. and Y Goto. Emissions suppression mechanism of premixed diesel combustion with variable valve timing. International Journal of Engine Research. October 2007 Vol 8 No 5. ISSN 1468-0874.

List figures

1. Experimental installation.
2. Control volume for zero-dimensional analysis
3. Cumulative heat release profile with net heat release calculated from the zero-dimensional model, Φ=0.35, fuel consumption of 0.015 g/cycle, 1800 RPM, 0% EGR and intake temperature of 18ºC.
4. Combustion chamber pressure versus crank angle with a compression ratio of 15:1, intake temperature of 18ºC, angular speed of 2100 RPM, initial Φ=0.48 and constant fuel consumption of 0.028 g/cycle for different EGR rates.
5. Combustion ignition angle and combustion duration as a function of EGR rate and fuel consumption with an intake temperature of 18ºC, compression ratio of 15:1, angular speed of 2100 RPM
6. Scheme of the optimization procedure
7. Measured and predicted cylinder pressure traces with a 1.3e-5kg/cycle of fuel consumption, 1800 RPM.
8. Measured and predicted cylinder pressure and HRR simulated in HCCI combustion mode (angular velocity is 2100 RPM, constant fuel consumption 2.75e-5 kg/cycle, initial Φ=0.57 and different EGR rate).

9. Measured and predicted cylinder pressure and HRR simulated in HCCI combustion mode (angular velocity is 1500 RPM, constant fuel consumption 1.8e-5 kg/cycle, initial Φ=0.3 and different EGR rate).

List tables

1. Deutz FL1 906 Engine characteristics.
2. The Best-fit parameters from new HRR law for different tests.
3. Accuracy of numeric model.

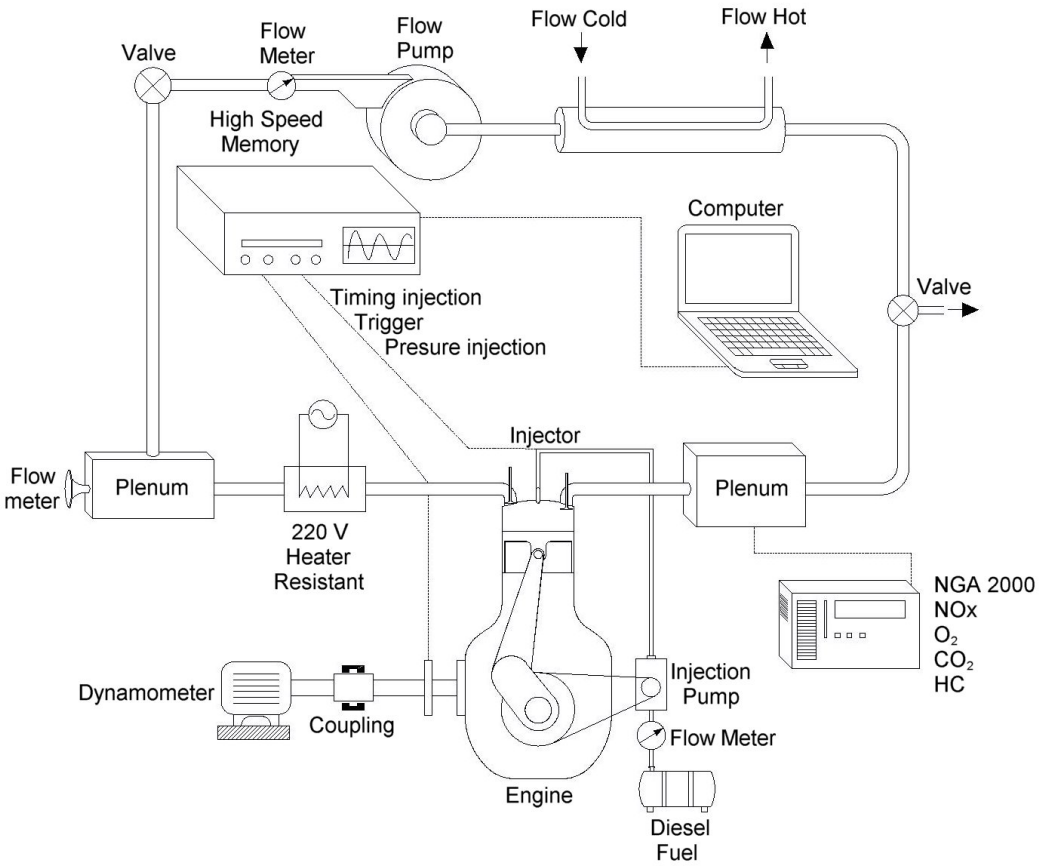

Figure 1. Experimental installation.

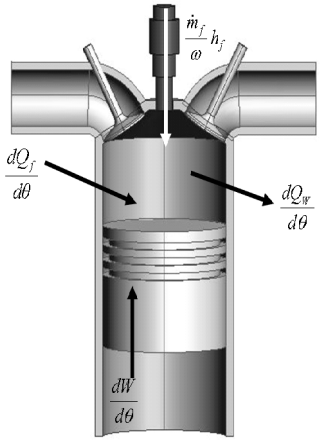

Figure 2. Control volume for zero-dimensional analysis

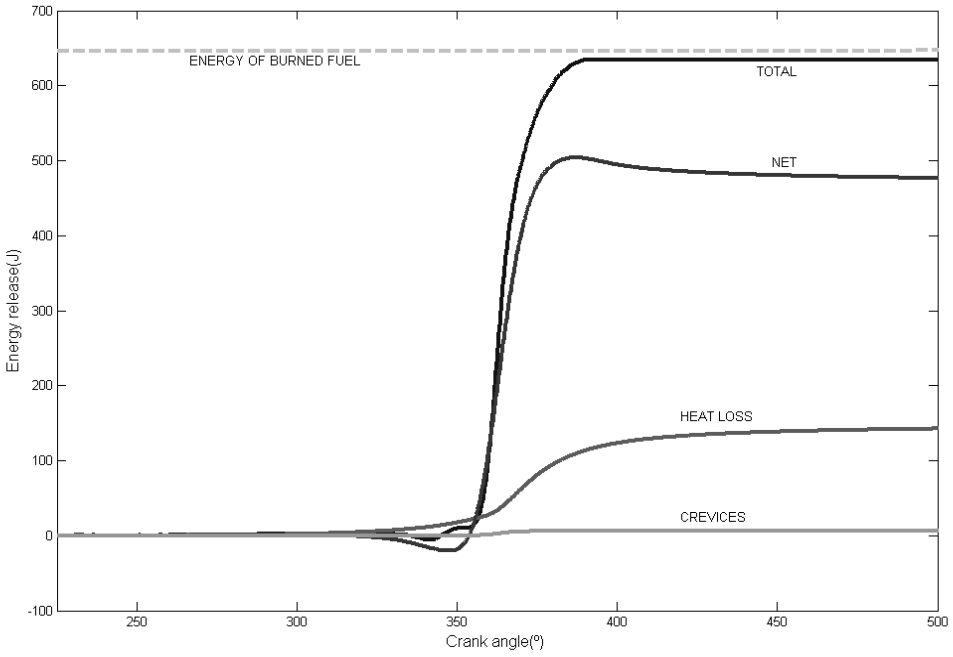

Figure 3 Cumulative heat release profile with net heat release calculated from the zero-dimensional model, Φ=0.35, fuel consumption of 0.015 g/cycle, 1800 RPM, 0% EGR and intake temperature of 18ºC.

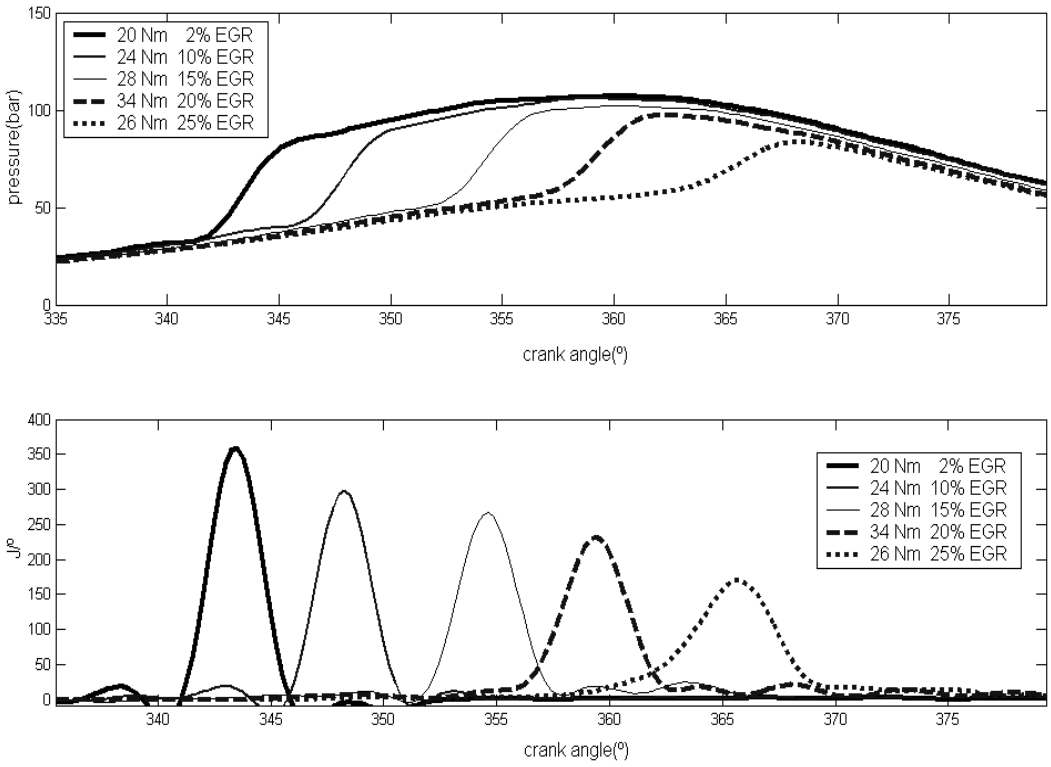

Figure 4 Combustion chamber pressure versus crank angle with a compression ratio of 15:1, intake temperature of 18ºC, angular speed of 2100 RPM, initial Φ=0.48 and constant fuel consumption of 0.028 g/cycle for different EGR rates.

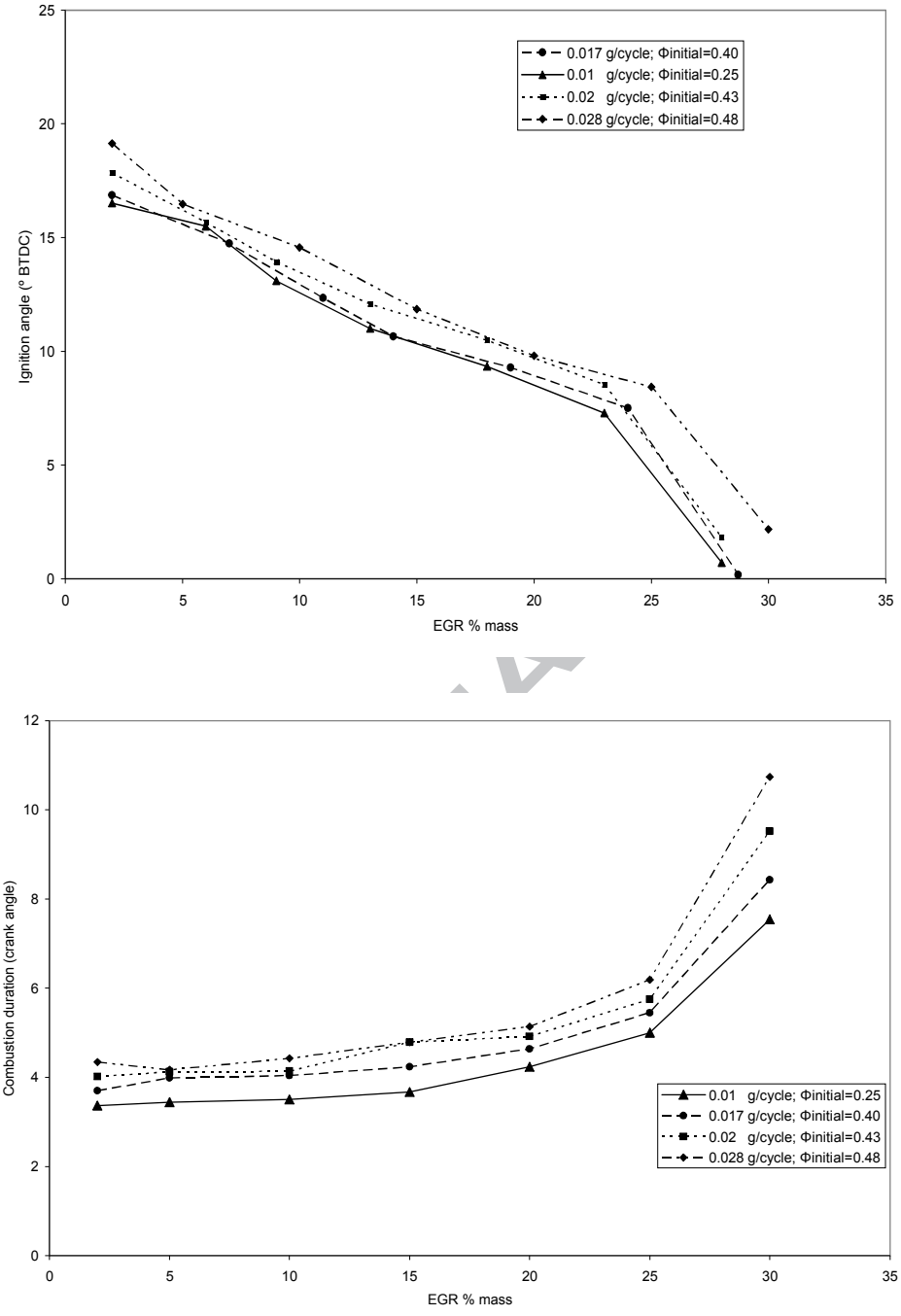

Figure 5 Combustion ignition angle and combustion duration as a function of EGR rate and fuel consumption with an intake temperature of 18ºC, compression ratio of 15:1, angular speed of 2100 RPM.

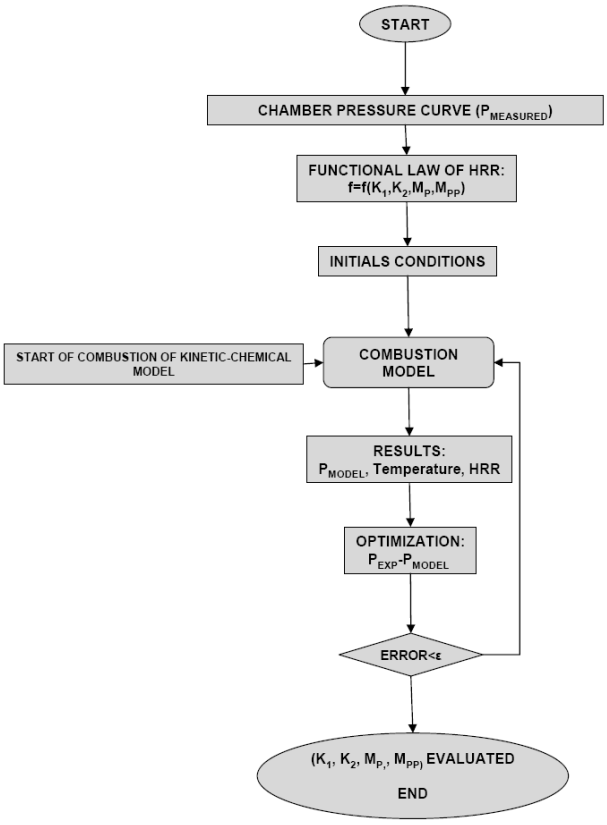

Figure 6. Scheme of the optimization procedure.

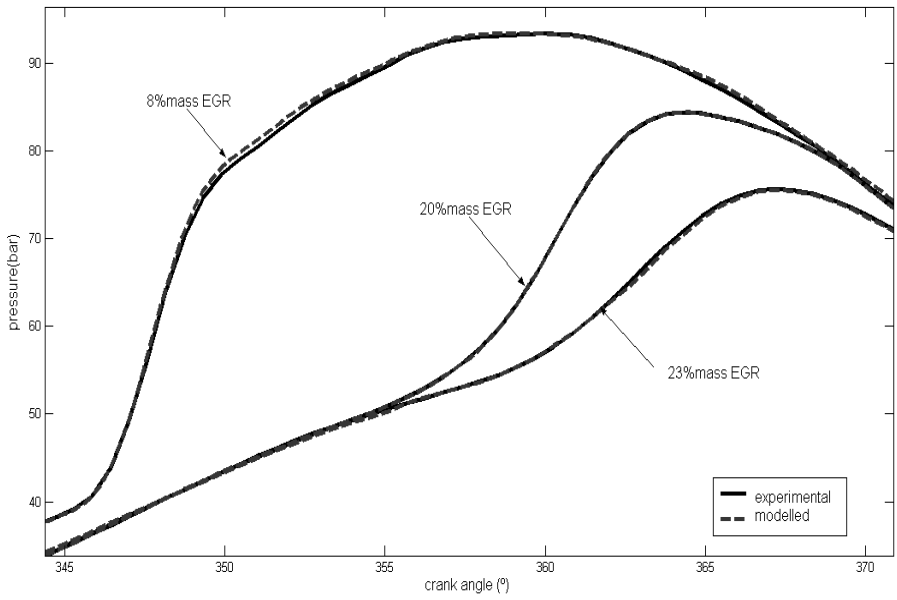

Figure 7. Measured and predicted cylinder pressure traces with a 1.3e-5kg/cycle of fuel

consumption, 1800 RPM.

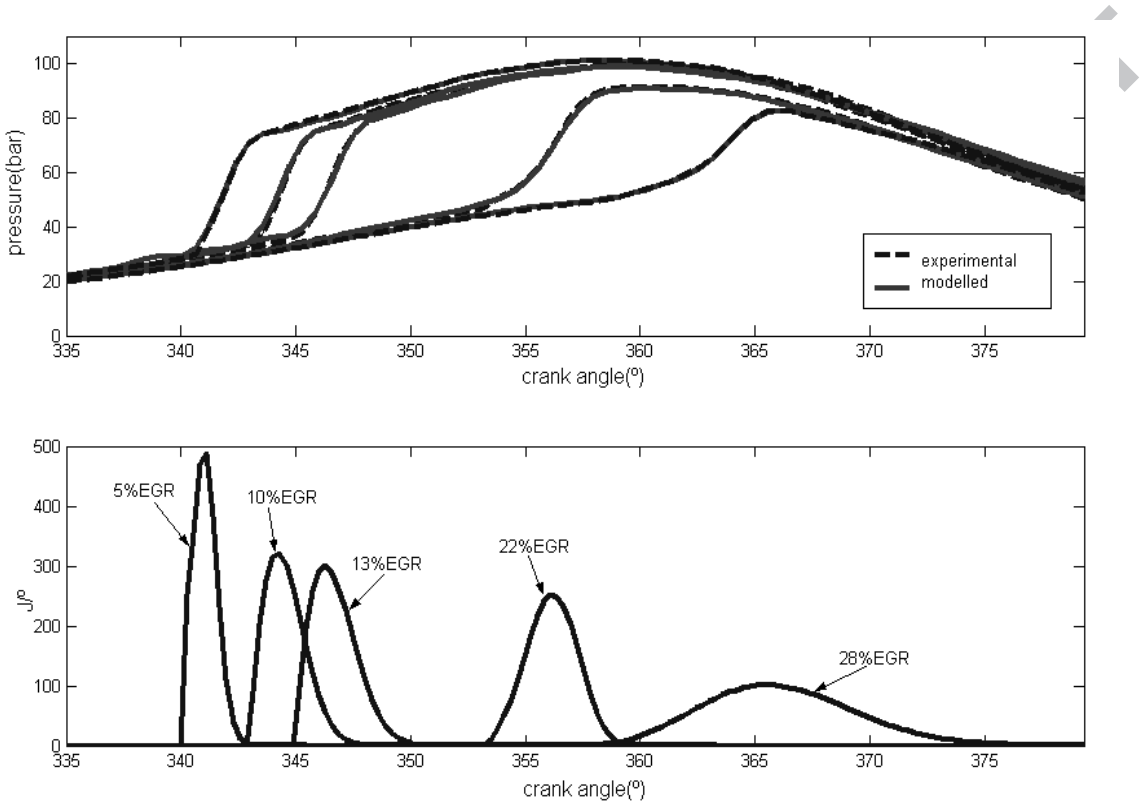

Figure 8. Measured and predicted cylinder pressure and HRR simulated in HCCI combustion mode (angular velocity is 2100 RPM, constant fuel consumption 2.75e-5 kg/cycle, initial Φ=0.57 and different EGR rate).

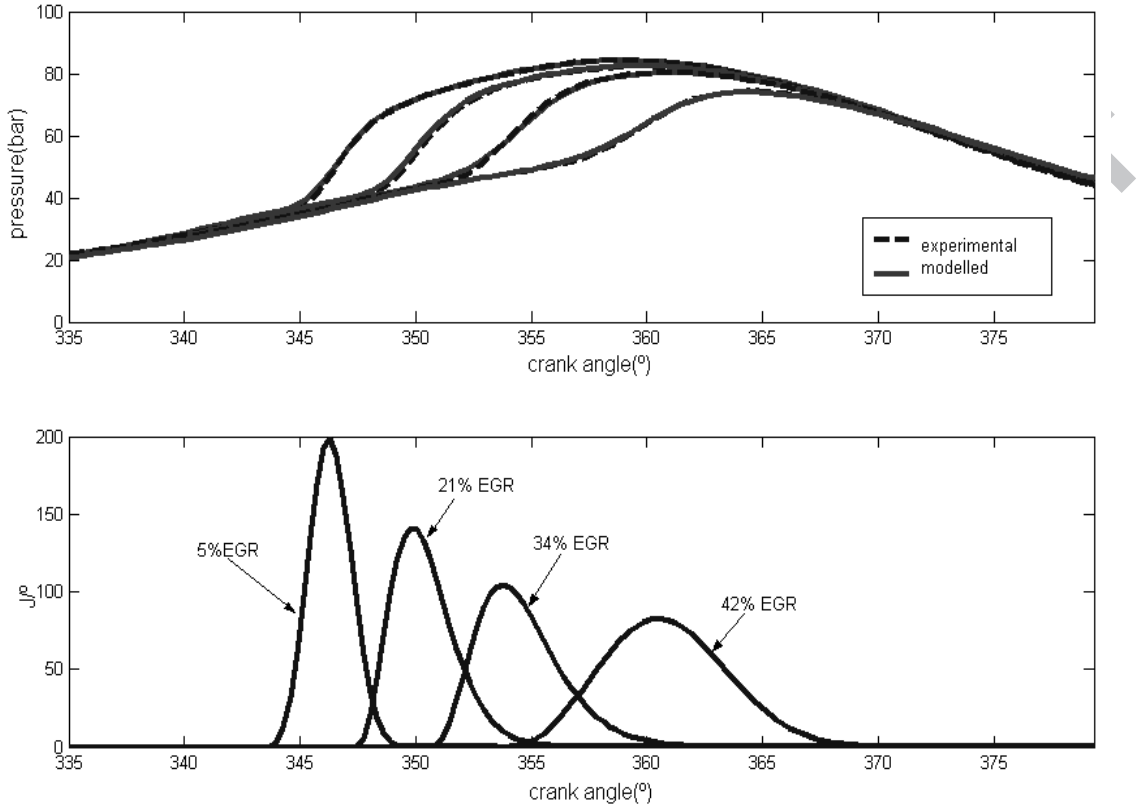

Figure 9. Measured and predicted cylinder pressure and HRR simulated in HCCI combustion mode (angular velocity is 1500 RPM, constant fuel consumption 1.8e-5 kg/cycle, initial Φ=0.3 and different EGR rate).

Table 1. Deutz FL1 906 Engine characteristics.

Type	DI Monocylinder 4 stroke
Cylinder displacement	708 cm^3
Bore	95 mm
Stroke	100 mm
Compression ratio	19:1

Maximum power	11 kW to 3000 RPM
Maximum torque	45 Nm to 2100 RPM
Fuel	Diesel
Lubricating	Gear oil
Injection pump	Mechanic
Refrigeration	Air

Table 2. The Best-fit parameters from new HRR law for different tests.

RPM	Fuel consumption (10^{-5} kg/cycle)	EGR % (mass)	K_1	K_2	M_p	M_{pp}
1350	1.24	35	54.7	0.28	0.76	2.65
1650	2.45	30	67.4	0.17	1.38	1.92
1800	2.98	28	98.4	2.89	2.55	1.15
2000	2.52	13	84.	0.26	1.98	1.61
2400	3.02	21	43.4	0.13	3.01	1.48
1200	1.74	38	75.3	0.037	0.51	1.40

Table 3. Accuracy of numeric model.

RPM	Torque (Nm)	m_f (10^{-5} kg/cycle)	% EGR (mass)	Error % Pressure maximum	Error % presusure area (total)*	Error % pressure area (parcial)**	Error ε rms (curve cylinder pressure)
1200	5	1.63	2	0.142	0.15	0.35	0.046
1200	10	1.63	47	-0.24	0.413	0.41	0.038
1200	10	2.19	2	0.03	-1.12	-1.25	0.047
1200	12	2.19	13	-0.11	-1.36	-1.65	0.274

1200	14	2.19	32	-0. 115	0.11	0.31	0.084
1200	15	2.90	2	-0.34	0.165	0.65	0.074
1200	17	2.90	12	-0.21	-0.44	-0.234	0.028
1200	22	2.90	32	-0.13	-1.83	-1.34	0.007
1200	26	2.90	42	-0.45	-0.34	-0.31	0.063
1200	20	3.60	2	0.324	0.45	0.54	0.03
1200	22	3.60	10	0.45	0.23	0.43	0.14
1200	25	3.60	15	0.53	-0.32	-0.58	0.095
1200	30	3.60	23	0.12	-0.31	-0.37	0.02
1500	5	1.51	2	-0.35	-0.53	-0.26	-0.18
1500	7	1.51	16	-0.09	0.65	0.29	0.05
1500	10	1.80	5	0.53	0.36	0.64	0.094
1500	14	1.80	21	0.87	0.43	0.74	-0.076
1500	16	1.80	34	0.29	0.67	0.48	0.08
1500	18	1.80	42	-0.54	-0.72	-0.38	-0.056
1500	15	2.55	5	0.43	-0.53	-0.64	0.35
1500	17	2.55	12	0.64	-0.55	-0.35	0.02
1500	20	2.55	22	0.72	0.45	0.75	0.03
1500	23	2.55	26	0.85	0.34	0.45	0.042
1800	5	1.41	2	0.52	0.36	0.45	0.027
1800	8	1.41	10	0.84	0.63	0.33	0.035

* Between IVC until EVO.

** from 35º BTDC until 35º ATDC.